Two-photon exchange in elastic electron-nucleon scattering

P. G. Blunden,[1] W. Melnitchouk,[2] and J. A. Tjon[2,3]
[1]*Department of Physics and Astronomy, University of Manitoba, Winnipeg, Manitoba, Canada R3T 2N2*
[2]*Jefferson Lab, 12000 Jefferson Ave., Newport News, Virginia 23606, USA*
[3]*Department of Physics, University of Maryland, College Park, Maryland 20742-4111, USA*
(Received 13 June 2005; published 30 September 2005)

A detailed study of two-photon exchange in unpolarized and polarized elastic electron-nucleon scattering is presented, taking particular account of nucleon finite size effects. Contributions from nucleon elastic intermediate states are found to have a strong angular dependence, which leads to a partial resolution of the discrepancy between the Rosenbluth and polarization transfer measurements of the proton electric to magnetic form factor ratio, G_E/G_M. The two-photon exchange contribution to the longitudinal polarization transfer P_L is small, whereas the contribution to the transverse polarization transfer P_T is enhanced at backward angles by several percent, increasing with Q^2. This gives rise to a small, $\lesssim 3\%$ suppression of G_E/G_M obtained from the polarization transfer ratio P_T/P_L at large Q^2. We also compare the two-photon exchange effects with data on the ratio of e^+p to e^-p cross sections, which is predicted to be enhanced at backward angles. Finally, we evaluate the corrections to the form factors of the neutron and estimate the elastic intermediate state contribution to the ^{3}He form factors.

DOI: 10.1103/PhysRevC.72.034612 PACS number(s): 25.30.Bf, 13.40.Gp, 12.20.Ds, 25.10.+s

I. INTRODUCTION

Electromagnetic form factors are fundamental observables that characterize the composite nature of the nucleon. Several decades of elastic form factor experiments with electron beams, including recent high-precision measurements at Jefferson Lab and elsewhere, have provided considerable insight into the detailed structure of the nucleon.

In the standard one-photon exchange (Born) approximation, the electromagnetic current operator is parametrized in terms of two form factors, usually taken to be the Dirac (F_1) and Pauli (F_2) form factors,

$$\Gamma^\mu = F_1(q^2)\gamma^\mu + \frac{i\sigma^{\mu\nu}q_\nu}{2M}F_2(q^2), \tag{1}$$

where q is the momentum transfer to the nucleon and M is the nucleon mass. The resulting cross section depends on two kinematic variables, conventionally taken to be $Q^2 \equiv -q^2$ (or $\tau \equiv Q^2/4M^2$) and either the scattering angle θ or the virtual photon polarization $\varepsilon = [1 + 2(1+\tau)\tan^2(\theta/2)]^{-1}$. In terms of the Sachs electric and magnetic form factors, defined as

$$G_E(Q^2) = F_1(Q^2) - \tau F_2(Q^2), \tag{2}$$

$$G_M(Q^2) = F_1(Q^2) + F_2(Q^2), \tag{3}$$

the reduced Born cross section can be written as follows:

$$\sigma_R = G_M^2(Q^2) + \frac{\varepsilon}{\tau}G_E^2(Q^2). \tag{4}$$

The standard method that has been used to determine the electric and magnetic form factors, particularly those of the proton, has been the Rosenbluth, or longitudinal-transverse (LT), separation method. Because the form factors in Eq. (4) are functions of Q^2 only, studying the cross section as a function of the polarization ε at fixed Q^2 allows one to extract G_M^2 from the ε-intercept and the ratio $R \equiv \mu G_E/G_M$ from the slope in ε, where μ is the nucleon magnetic moment. The results of the Rosenbluth measurements for the proton have generally been consistent with $R \approx 1$ for $Q^2 \lesssim 6$ GeV^2 [1–3]. The "Super-Rosenbluth" experiment at Jefferson Lab [4], in which smaller systematic errors were achieved by detecting the recoiling proton rather than the electron, as in previous measurements, is also consistent with the earlier LT results.

An alternative method of extracting the ratio R has been used recently at Jefferson Lab [5], in which a polarized electron beam scatters from an unpolarized target, with measurement of the polarization of the recoiling proton. From the ratio of the transverse to longitudinal recoil polarizations one finds

$$R = -\mu\frac{E_1+E_3}{2M}\tan\frac{\theta}{2}\frac{P_T}{P_L} = -\mu\sqrt{\frac{\tau(1+\varepsilon)}{2\varepsilon}}\frac{P_T}{P_L}, \tag{5}$$

where E_1 and E_3 are the initial and final electron energies and P_T (P_L) is the polarization of the recoil proton transverse (longitudinal) to the proton momentum in the scattering plane. The polarization transfer experiments yielded strikingly different results compared with the LT separation, with $R \approx 1 - 0.135(Q^2/\mathrm{GeV}^2 - 0.24)$ over the same range in Q^2 [2]. Recall that in perturbative quantum chromodynamics (QCD) one expects $F_1 \sim Q^2 F_2$ at large Q^2 (or equivalently $G_E \sim G_M$) [6], so that these results imply a strong violation of scaling behavior (see also Refs. [7,8]).

The question of which experiments are correct has been debated over the past several years. Attempts to reconcile the different measurements have been made by several authors [9–12], who considered whether 2γ exchange effects, which form part of the radiative corrections (RCs) and which are treated in an approximate manner in the standard RC calculations [13], could account for the observed discrepancy. An explicit calculation [10] of the two-photon exchange diagram, in which nucleon structure effects were for the first time fully incorporated, indeed showed that around half of the discrepancy could be removed just by the nucleon elastic intermediate states. A partonic level calculation [11,12] subsequently showed that the deep inelastic region can also contribute significantly to the box diagram.

In this article we further develop the methodology introduced in Ref. [10] and apply it to systematically calculate the 2γ exchange effects in a number of electron-nucleon scattering observables. We focus on the nucleon elastic intermediate states; inelastic contributions are discussed elsewhere [14]. In Sec. II we examine the effects of 2γ exchange on the ratio of electric to magnetic form factors in unpolarized scattering. In contrast to the earlier analysis [10], in which simple monopole form factors were utilized at the internal γNN vertices, here we parameterize the vertices by realistic form factors and study the model dependence of effects on the ratio R because of the choice of form factors. We also compare the results with data on the ratio of e^+p to e^-p scattering cross sections, which is directly sensitive to 2γ exchange effects.

In Sec. III we examine the effects of 2γ exchange on the polarization transfer reaction, $\vec{e}p \to e\vec{p}$, for both longitudinally and transversely polarized recoil protons. We also consider the case of proton polarization normal to the reaction plane, which depends on the imaginary part of the box diagram. Because this is absent in the Born approximation, the normal polarization provides a clean signature of 2γ exchange effects, even though it does not directly address the G_E^p/G_M^p discrepancy. Following the discussion of the proton, in Sec. IV we consider 2γ exchange corrections to the form factors of the neutron, both for the LT separation and polarization transfer techniques. Applying the same formalism to the case of the ^{3}He nucleus, in Sec. V we compute the elastic contribution from the box diagram to the ratio of charge to magnetic form factors of ^{3}He. In Sec. VI we summarize our findings, and discuss future work.

II. TWO-PHOTON EXCHANGE IN UNPOLARIZED SCATTERING

In this section we outline the formalism used to calculate the 2γ exchange contribution to the unpolarized electron-nucleon cross section and examine the effect on the G_E^p/G_M^p ratio extracted using LT separation. Because there are in general three form factors that are needed to describe elastic eN scattering beyond 1γ exchange, we also evaluate the 2γ contributions to each of the form factors separately. In the final part of this section, we examine the effect of the 2γ correction on the ratio of e^+p to e^-p elastic cross sections, which is directly sensitive to 2γ exchange effects.

A. Formalism

For the elastic scattering process we define the momenta of the initial electron and nucleon as p_1 and p_2 and of the final electron and nucleon as p_3 and p_4, respectively, $e(p_1) + p(p_2) \to e(p_3) + p(p_4)$. The four-momentum transferred from the electron to the nucleon is given by $q = p_4 - p_2 = p_1 - p_3$ (with $Q^2 \equiv -q^2 > 0$), and the total electron and proton invariant mass squared is given by $s = (p_1 + p_2)^2 = (p_3 + p_4)^2$. In the Born approximation, the amplitude can be written as

$$\mathcal{M}_0 = -i\frac{e^2}{q^2}\bar{u}(p_3)\gamma_\mu u(p_1)\,\bar{u}(p_4)\Gamma^\mu(q)u(p_2), \tag{6}$$

where e is the electron charge, and Γ^μ is given by Eq. (1). In terms of the amplitude $\mathcal{M}_0$, the corresponding differential Born cross section is given by

$$\frac{d\sigma_0}{d\Omega} = \left(\frac{\alpha}{4Mq^2}\frac{E_3}{E_1}\right)^2 |\mathcal{M}_0|^2 = \sigma_{\text{Mott}}\frac{\tau}{\varepsilon(1+\tau)}\sigma_R, \tag{7}$$

where σ_R is the reduced cross section given in Eq. (4), and the Mott cross section for the scattering from a point particle is

$$\sigma_{\text{Mott}} = \frac{\alpha^2 E_3 \cos^2\frac{\theta}{2}}{4E_1^3\sin^4\frac{\theta}{2}}, \tag{8}$$

with E_1 and E_3 the initial and final electron energies and $\alpha = e^2/4\pi$ the electromagnetic fine structure constant. Including radiative corrections to order α, the elastic scattering cross section is modified as follows:

$$\frac{d\sigma_0}{d\Omega} \to \frac{d\sigma}{d\Omega}(1+\delta), \tag{9}$$

where δ includes one-loop virtual corrections (vacuum polarization, electron and proton vertex, and two photon exchange corrections), as well as inelastic bremsstrahlung for real photon emission [13].

According to the LT separation technique, one extracts the ratio R^2 from the ε dependence of the cross section at fixed Q^2. Because of the factor ε/τ multiplying G_E^2 in Eq. (4), the cross section becomes dominated by G_M^2 with increasing Q^2, whereas the relative contribution of the G_E^2 term is suppressed. Hence understanding the ε dependence of the radiative correction δ becomes increasingly important at high Q^2. As pointed out in Ref. [2], for example, a few-percent change in the ε slope in $d\sigma$ can lead to a sizable effect on R. In contrast, as we discuss in Sec. III below, the polarization transfer technique does not show the same sensitivity to the ε dependence of δ.

If we denote the amplitude for the one-loop virtual corrections by $\mathcal{M}_1$, then $\mathcal{M}_1$ can be written as the sum of a "factorizable" term, proportional to the Born amplitude $\mathcal{M}_0$, and a nonfactorizable part $\overline{\mathcal{M}}_1$,

$$\mathcal{M}_1 = f(Q^2,\varepsilon)\mathcal{M}_0 + \overline{\mathcal{M}}_1. \tag{10}$$

The ratio of the full cross section (to order α) to the Born can therefore be written as

$$1+\delta = \frac{|\mathcal{M}_0 + \mathcal{M}_1|^2}{|\mathcal{M}_0|^2}, \tag{11}$$

with δ given by

$$\delta = 2f(Q^2,\varepsilon) + \frac{2\mathcal{R}e\{\mathcal{M}_0^\dagger\overline{\mathcal{M}}_1\}}{|\mathcal{M}_0|^2}. \tag{12}$$

In practice the factorizable terms parametrized by $f(Q^2,\varepsilon)$, which includes the electron vertex correction, vacuum polarization, and the infrared (IR) divergent parts of the nucleon vertex and two-photon exchange corrections, are found to be dominant. Furthermore, these terms are all essentially independent of hadronic structure.

However, as explained in Ref. [10], the contributions to the functions $f(Q^2, \varepsilon)$ from the electron vertex, vacuum polarization, and proton vertex terms depend only on Q^2 and therefore have no relevance for the LT separation aside from an overall normalization factor. Hence, of the factorizable terms, only the IR divergent two-photon exchange contributes to the ε dependence of the virtual photon corrections.

The terms that do depend on hadronic structure are contained in $\overline{\mathcal{M}_1}$ and arise from the finite nucleon vertex and two-photon exchange corrections. For the case of the proton, the hadronic vertex correction was analyzed by Maximon and Tjon [15] and found to be <0.5% for $Q^2 < 6$ GeV^2. Because of the proton vertex correction does not have a strong ε dependence, it will not affect the LT analysis and can be safely neglected.

For the inelastic bremsstrahlung cross section, the amplitude for real photon emission can also be written in the form of Eq. (10). In the soft photon approximation the amplitude is completely factorizable. A significant ε dependence arises because of the frame dependence of the angular distribution of the emitted photon. These corrections, together with external bremsstrahlung, contain the main ε dependence of the radiative corrections and are usually accounted for in the experimental analyses. They are generally well understood and in fact enter differently depending on whether the electron or proton are detected in the final state. Hence corrections beyond the standard $\mathcal{O}(\alpha)$ radiative corrections that can lead to nonnegligible ε dependence are confined to the 2γ exchange diagrams, illustrated in Fig. 1, and are denoted by $\mathcal{M}^{2\gamma}$, which we focus on in the following. The 2γ exchange correction $\delta^{2\gamma}$ we calculate is then essentially as follows:

$$\delta^{2\gamma} \to \frac{2\mathcal{R}e\{\mathcal{M}_0^\dagger \mathcal{M}^{2\gamma}\}}{|\mathcal{M}_0|^2}. \tag{13}$$

In principle the two-photon exchange amplitude $\mathcal{M}^{2\gamma}$ includes all possible hadronic intermediate states in Fig. 1. Here we consider only the elastic contribution to the full response function and assume that the proton propagates as a Dirac particle (excited state contributions are considered in Ref. [14]). We also assume that the structure of the off-shell current operator is similar to that in Eq. (1) and use phenomenological form factors at the γNN vertices. This is of course the source of the model dependence in the problem. Clearly this is circular, as the radiative corrections are also used to determine the experimental form factors. However, because δ is a ratio, the model dependence cancels somewhat,

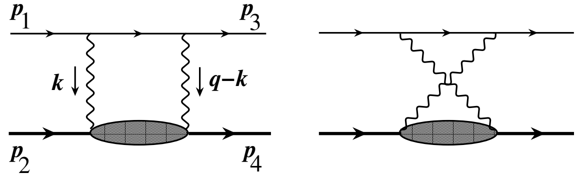

FIG. 1. Two-photon exchange box and crossed box diagrams for elastic electron-proton scattering.

provided the same phenomenological form factors are used for both $\mathcal{M}_0$ and $\mathcal{M}^{2\gamma}$ in Eq. (13).

The total 2γ exchange amplitude, including the box and crossed box diagrams in Fig. 1, has the form

$$\mathcal{M}^{2\gamma} = e^4 \int \frac{d^4k}{(2\pi)^4} \frac{N_{\text{box}}(k)}{D_{\text{box}}(k)} + e^4 \int \frac{d^4k}{(2\pi)^4} \frac{N_{\text{x-box}}(k)}{D_{\text{x-box}}(k)}, \tag{14}$$

where the numerators are the matrix elements

$$\begin{aligned} N_{\text{box}}(k) = {}& \bar{u}(p_3)\gamma_\mu(\not{p}_1 - \not{k} + m)\gamma_\nu u(p_1)\bar{u}(p_4)\Gamma^\mu(q-k) \\ & \times (\not{p}_2 + \not{k} + M)\Gamma^\nu(k)u(p_2), \end{aligned} \tag{15}$$

$$\begin{aligned} N_{\text{x-box}}(k) = {}& \bar{u}(p_3)\gamma_\nu(\not{p}_3 + \not{k} + m)\gamma_\mu u(p_1)\bar{u}(p_4)\Gamma^\mu(q-k) \\ & \times (\not{p}_2 + \not{k} + M)\Gamma^\nu(k)u(p_2), \end{aligned} \tag{16}$$

and the denominators are products of propagators

$$\begin{aligned} D_{\text{box}}(k) = {}& [k^2 - \lambda^2][(k-q)^2 - \lambda^2] \\ & \times [(p_1 - k)^2 - m^2][(p_2 + k)^2 - M^2], \end{aligned} \tag{17}$$

$$D_{\text{x-box}}(k) = D_{\text{box}}(k)|_{p_1 - k \to p_3 + k} \, . \tag{18}$$

An infinitesimal photon mass λ has been introduced in the photon propagator to regulate the IR divergences. The IR divergent part is of interest because it is the one usually included in the standard RC analyses. The finite part, which is typically neglected, has been included in Ref. [10] and found to have significant ε dependence.

The IR divergent part of the amplitude $\mathcal{M}^{2\gamma}$ can be separated from the IR finite part by analyzing the structure of the photon propagators in the integrand of Eq. (14). The two poles, where the photons are soft, occur at $k = 0$ and at $k = q$. The dominant (IR divergent) contribution to the integral (14) comes from the poles, and one therefore typically makes the following approximation:

$$\begin{aligned} \mathcal{M}_{\text{IR}}^{2\gamma} \approx {}& e^4 N_{\text{box}}(0) \int \frac{d^4k}{(2\pi)^4} \frac{1}{D_{\text{box}}(k)} + e^4 N_{\text{x-box}}(0) \\ & \times \int \frac{d^4k}{(2\pi)^4} \frac{1}{D_{\text{x-box}}(k)}, \end{aligned} \tag{19}$$

with

$$N_{\text{box}}(q) = N_{\text{box}}(0) = 4ip_1 \cdot p_2 \frac{q^2 \mathcal{M}_0}{e^2}, \tag{20}$$

$$N_{\text{x-box}}(q) = N_{\text{x-box}}(0) = 4ip_3 \cdot p_2 \frac{q^2 \mathcal{M}_0}{e^2}. \tag{21}$$

In this case the IR divergent contribution is proportional to the Born amplitude, and the corresponding correction to the Born cross section is independent of hadronic structure.

The remaining integrals over propagators can be done analytically. In the target rest frame the total IR divergent two-photon exchange contribution to the cross section is found to be

$$\delta_{\text{IR}} = -\frac{2\alpha}{\pi} \ln\left(\frac{E_1}{E_3}\right) \ln\left(\frac{Q^2}{\lambda^2}\right), \tag{22}$$

a result given by Maximon and Tjon [15]. The logarithmic IR singularity in λ is exactly canceled by a corresponding term in the bremsstrahlung cross section involving the interference between real photon emission from the electron and from the nucleon.

By contrast, in the standard treatment of Mo and Tsai (MT) [13] a different approximation for the integrals over propagators is introduced. Here, the IR divergent contribution to the cross section is

$$\delta_{\rm IR}({\rm MT}) = -2\frac{\alpha}{\pi}\left[K(p_1,p_2) - K(p_3,p_2)\right], \tag{23}$$

where $K(p_i,p_j) = p_i \cdot p_j \int_0^1 dy\, \ln(p_y^2/\lambda^2)/p_y^2$ and $p_y = p_i y + p_j(1-y)$. The logarithmic dependence on λ is the same as Eq. (22), however.

As mentioned above, the full expression in Eq. (14) includes both finite and IR divergent terms and form factors at the γNN vertices. In Ref. [10] the proton form factors F_1 and F_2 were expressed in terms of the Sachs electric and magnetic form factors,

$$F_1(Q^2) = \frac{G_E(Q^2) + \tau G_M(Q^2)}{1+\tau}, \tag{24}$$

$$F_2(Q^2) = \frac{G_M(Q^2) - G_E(Q^2)}{1+\tau}, \tag{25}$$

with G_E and G_M both parametrized by a simple monopole form, $G_{E,M}(Q^2) \sim \Lambda^2/(\Lambda^2+Q^2)$, with the mass parameter Λ related to the size of the proton. In the present analysis we generalize this approach by using more realistic form factors in the loop integration, consistent with the actual $G_{E,M}$ data. The functions F_1 and F_2 are parametrized directly in terms of sums of monopoles, of the form

$$F_{1,2}(Q^2) = \sum_{i=1}^{N} \frac{n_i}{d_i + Q^2}, \tag{26}$$

where n_i and d_i are free parameters, and n_N is determined from the normalization condition, $n_N = d_N[F_{1,2}(0) - \sum_{i=1}^{N-1} n_i/d_i]$. The parameters n_i and d_i for the F_1 and F_2 form factors of the proton and neutron are given in Table I. The normalization conditions are $F_1^p(0) = 1$ and $F_2^p(0) = \kappa_p$ for the proton and $F_1^n(0) = 0$ and $F_2^n(0) = \kappa_n$ for the neutron, where $\kappa_p = 1.793$ and $\kappa_n = -1.913$ are the proton and neutron anomalous magnetic moments, respectively.

In practice we use the parametrization from Ref. [16] and fit the parametrized form factors as a sum of three monopoles, except for F_2^n, which is fitted with $N = 2$. As discussed in the next section, the sensitivity of the results to the choice of form factor is relatively mild. Of course, one should note that the data to which the form factors are fitted were extracted under the assumption of 1γ exchange, so that in principle one should iterate the data extraction and fitting procedure for self-consistency. However, within the accuracy of the data and of the 2γ calculation the effect of this will be small.

TABLE I. Parameters for the proton and neutron form factor fits in Eq. (26) used in this work, with n_i and d_i in units of GeV^2.

N	F_1^p	F_2^p	F_1^n	F_2^n
	3	3	3	2
n_1	0.38676	1.01650	24.8109	5.37640
n_2	0.53222	–19.0246	–99.8420	
d_1	3.29899	0.40886	1.98524	0.76533
d_2	0.45614	2.94311	1.72105	0.59289
d_3	3.32682	3.12550	1.64902	—

To obtain the radiatively corrected cross section for unpolarized electron scattering the polarizations of the incoming and outgoing electrons and nucleons in Eqs. (15) and (16) need to be averaged and summed, respectively. The resulting expression involves a product of traces in the Dirac spaces of the electron and nucleon. The trace algebra is tedious but straightforward. It was carried out using the algebraic program FORM [17] and verified independently using the program Tracer [18]. We also used two independent Mathematica packages (FeynCalc [19] and FormCalc [20]) to carry out the loop integrals. The packages gave distinct but equivalent analytic expressions, which gave identical numerical results. The loop integrals in Eq. (14) can be expressed in terms of 4-point Passarino-Veltman functions [21], which have been calculated using Spence functions [22] as implemented by Veltman [23]. In the actual calculations we have used the FF program [24]. The results of the proton calculation are presented in the following section.

B. 2γ corrections to proton form factors

In typical experimental analyses of electromagnetic form factor data [1] radiative corrections are implemented using the prescription of Ref. [13], including using Eq. (23) to approximate the 2γ contribution. To investigate the effect of our results on the data analyzed in this manner, we therefore compare the ε dependence of the full calculation with that of $\delta_{\rm IR}({\rm MT})$. To make the comparison meaningful, we will consider the difference

$$\Delta \equiv \delta_{\rm full} - \delta_{\rm IR}({\rm MT}), \tag{27}$$

in which the IR divergences cancel, and which is independent of λ.

The results for the difference Δ between the full calculation and the MT approximation are shown in Fig. 2 for several values of Q^2 from 1 to 6 GeV^2. The additional corrections are most significant at low ε and essentially vanish at large ε. At the lower Q^2 values Δ is approximately linear in ε, but significant deviations from linearity are observed with increasing Q^2, especially at smaller ε.

In Fig. 3(a) we illustrate the model dependence of the results by comparing the results in Fig. 2 at $Q^2 = 1$ and 6 GeV^2 with those obtained using a dipole form for the F_1^p and F_2^p form factors, with mass $\Lambda = 0.84$ GeV. At the lower, $Q^2 = 1$ GeV^2, value the model dependence is very weak, with essentially no change at all in the slope. For the larger value $Q^2 = 6$ GeV^2 the differences are slightly larger, but the general trend of the correction remains unchanged. We can conclude therefore that the model dependence of the calculation is quite modest. Also displayed is the correction at $Q^2 = 12$ GeV^2, which will be accessible in future experiments, showing significant deviations from linearity over the entire ε range.

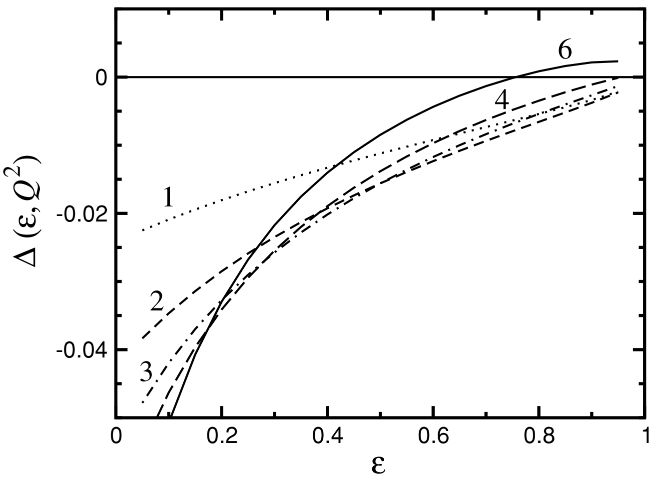

FIG. 2. Difference between the full two-photon exchange correction to the elastic cross section [using the realistic form factors in Eq. (26)] and the commonly used expression (23) from Ref. [13] for $Q^2 = 1$–6 GeV^2. The numbers labeling the curves denote the respective Q^2 values in GeV^2.

The results are also relatively insensitive to the high-Q^2 behavior of the G_E^p/G_M^p ratio, as Fig. 3(b) illustrates. Here the correction Δ is shown at $Q^2 = 6$ GeV^2 calculated using various form factor inputs, from parametrizations obtained by fitting only the LT-separated data [16,25], and those in which G_E^p is constrained by the polarization transfer data [25,26]. (Note that the G_M^p form factor itself also differs by a few percent between the various parametrizations.) The various curves are almost indistinguishable, and the dependence on the form factor inputs at lower Q^2 is expected to be even weaker than that in Fig. 3(b).

The effect of the 2γ corrections on the cross sections can be seen in Fig. 4, where the reduced cross-section σ_R, scaled by the square of the dipole form factor,

$$G_D = \left[1 + \frac{Q^2}{(0.84\ \mathrm{GeV})^2}\right]^{-2}, \tag{28}$$

is plotted as a function of ε for several fixed values of Q^2. In Fig. 4(a) the results are compared with the SLAC data [27] at $Q^2 = 3.25$, 4, 5 and 6 GeV^2 and with data from the “Super-Rosenbluth” experiment at JLab [4] in Fig. 4(b). In both cases the Born level results (dotted curves), which are obtained using the form factor parametrization of Ref. [26] in which G_E^p is fitted to the polarization transfer data [5], have slopes that are significantly shallower than the data. With the inclusion of the 2γ contribution (solid curves), there is a clear increase of the slope, with some nonlinearity evident at small ε. The corrected results are clearly in better agreement with the data although do not reproduce the entire correction necessary to reconcile the Rosenbluth and polarization transfer measurements.

To estimate the influence of these corrections on the electric to magnetic proton form factor ratio, the simplest approach is to examine how the ε slope changes with the inclusion of the 2γ exchange. Of course, such a simplified analysis can only be approximate because the ε dependence is linear only over

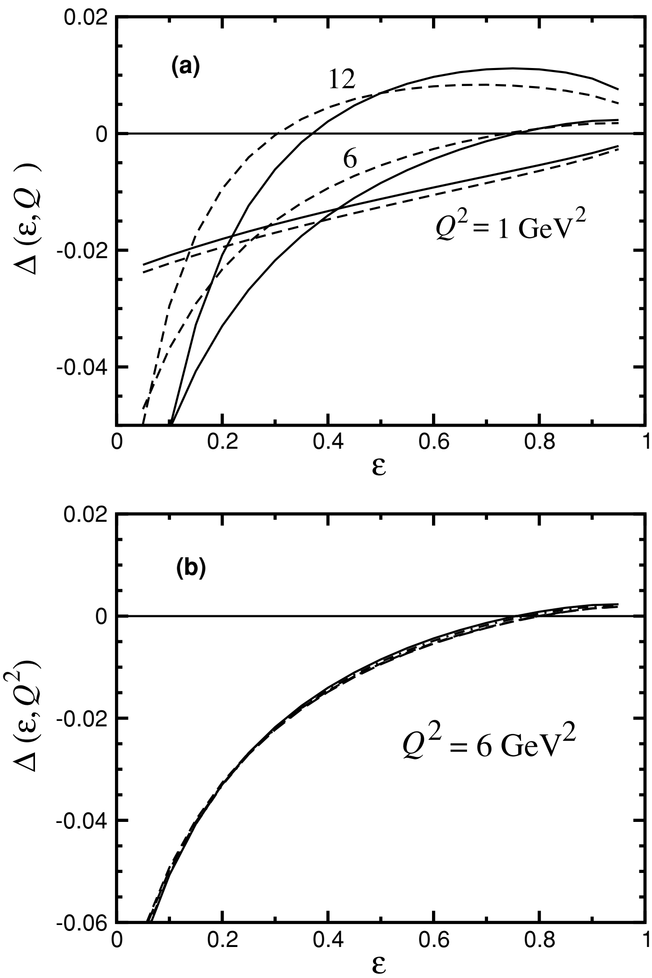

FIG. 3. Model dependence of the difference between the full two-photon exchange correction and the Mo and Tsai approximation: (a) at $Q^2 = 1$, 6, and 12 GeV^2, using realistic (solid) [16] and dipole (dashed) form factors; (b) at $Q^2 = 6$ GeV^2 using the form factor parametrizations from Refs. [16] (solid), [26] (dashed), and [25] with G_E^p constrained by the LT-separated (dot-dashed) and polarization transfer (long-dashed) data.

limited regions of ε, with clear deviations from linearity at low ε and high Q^2. In the actual data analyses one should apply the correction Δ directly to the data, as in Fig. 4. However, it is still instructive to obtain an estimate of the effect on R by taking the slope over several ranges of ε.

Following Ref. [10], this can be done by fitting the correction $(1 + \Delta)$ to a linear function of ε, of the form $a + b\varepsilon$, for each value of Q^2 at which the ratio R is measured. The corrected reduced cross section in Eq. (4) then becomes

$$\sigma_R \approx a G_M^2(Q^2)\left[1 + \frac{\varepsilon}{\mu^2\tau}(R^2\,[1 + \varepsilon b/a] + \mu^2\tau b/a)\right], \tag{29}$$

where

$$R^2 = \frac{\widetilde{R}^2 - \mu^2\tau b/a}{1 + \bar{\varepsilon} b/a} \tag{30}$$

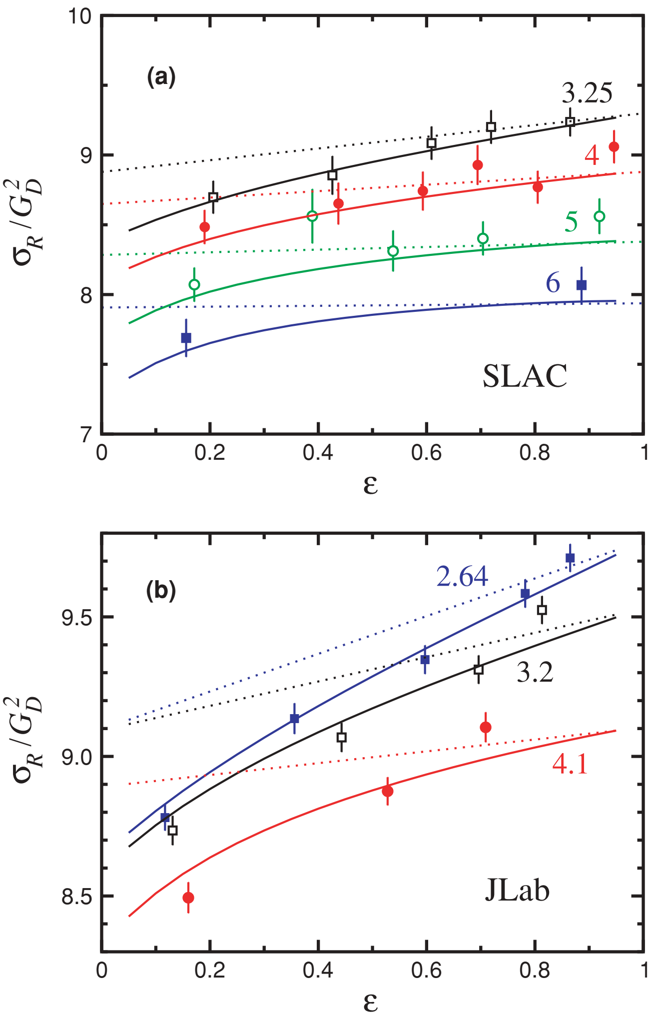

FIG. 4. (Color online) Reduced cross section σ_R (scaled by the dipole form factor G_D^2) versus ε for several values of Q^2: (a) SLAC data [27] at $Q^2 = 3.25$ (open squares), 4 (filled circles), 5 (open circles), and 6 GeV^2 (filled squares); (b) JLab data [4] at $Q^2 = 2.64$ (filled squares), 3.2 (open squares), and 4.1 GeV^2 (filled circles). The dotted curves are Born cross sections evaluated using a form factor parametrization [26] with G_E^p fitted to the polarization transfer data [5], whereas the solid curves include 2γ contributions. The curves in the bottom panel have been shifted by (+1.0%, +2.1%, +3.0%) for $Q^2 = (2.64, 3.2, 4.1)$ GeV^2.

is the "true" form factor ratio, corrected for 2γ exchange effects, and $\widetilde{R}$ is the "effective" ratio, contaminated by 2γ exchange. Note that in Eqs. (29) and (30) we have effectively linearized the quadratic term in ε by taking the average value of ε (i.e., $\bar{\varepsilon}$) over the ε range being fitted. In contrast to Ref. [10], where the approximation $a \approx 1$ was made and the quadratic term in ε neglected, the use of the full expression in Eq. (30) leads to a small decrease in R compared with the approximate form.

The shift in R is shown in Fig. 5, together with the polarization transfer data. We consider two ranges for ε: a large range $\varepsilon = 0.2$–0.9 and a more restricted range $\varepsilon = 0.5$–0.8. The approximation of linear ε dependence of Δ should be better for the latter, even though in practice experiments

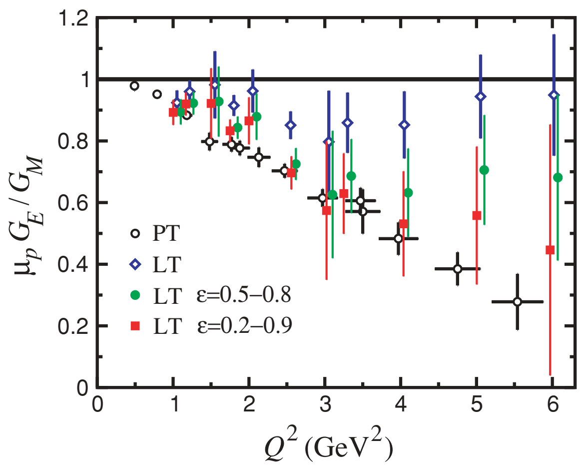

FIG. 5. (Color online) The ratio of proton form factors $\mu_p G_E/G_M$ measured using LT separation (open diamonds) [2] and polarization transfer (PT) (open circles) [5]. The LT points corrected for 2γ exchange are shown assuming a linear slope for $\varepsilon = 0.2$–0.9 (filled squares) and $\varepsilon = 0.5$–0.8 (filled circles) (offset for clarity).

typically sample values of ε near its lower and upper bounds. A proposed experiment at Jefferson Lab [28] aims to test the linearity of the ε plot through a precision measurement of the unpolarized elastic cross section.

The effect of the 2γ exchange terms on R is clearly significant. As observed in Ref. [10], the 2γ corrections have the proper sign and magnitude to resolve a large part of the discrepancy between the two experimental techniques. In particular, the earlier results [10] using simple monopole form factors found a shift similar to that for the $\varepsilon = 0.5$–0.8 range in Fig. 5, which resolves around 1/2 of the discrepancy. The nonlinearity at small ε makes the effective slope somewhat larger if the ε range is taken between 0.2 and 0.9. The magnitude of the effect in this case is sufficient to bring the LT and polarization transfer points almost to agreement, as indicated in Fig. 5.

Although the 2γ corrections clearly play a vital role in resolving most of the form factor discrepancy, it is instructive to understand the origin of the effect on R with respect to contributions to the individual G_E^p and G_M^p form factors. In general the amplitude for elastic scattering of an electron from a proton, beyond the Born approximation, can be described by three (complex) form factors, $\widetilde{F}_1$, $\widetilde{F}_2$, and $\widetilde{F}_3$. The generalized amplitude can be written as [9,11]

$$\mathcal{M} = -i\frac{e^2}{q^2}\bar{u}(p_3)\gamma_\mu u(p_1)\,\bar{u}(p_4) \times \left(\widetilde{F}_1\gamma^\mu + \widetilde{F}_2\frac{i\sigma^{\mu\nu}q_\nu}{2M} + \widetilde{F}_3\frac{\gamma\cdot K P^\mu}{M^2}\right)u(p_2), \quad (31)$$

where $K = (p_1 + p_3)/2$ and $P = (p_2 + p_4)/2$. The functions $\widetilde{F}_i$ (both real and imaginary parts) are in general functions of Q^2 and ε. In the 1γ exchange limit the $\widetilde{F}_{1,2}$ functions approach the usual (real) Dirac and Pauli form factors, whereas the new form factor $\widetilde{F}_3$ exists only at the 2γ level and beyond,

$$\widetilde{F}_{1,2}(Q^2, \varepsilon) \to F_{1,2}(Q^2), \quad (32)$$

$$\widetilde{F}_3(Q^2, \varepsilon) \to 0. \quad (33)$$

Alternatively, the amplitude can be expressed in terms of the generalized (complex) Sachs electric and magnetic form factors, $\widetilde{G}_E = G_E + \delta G_E$ and $\widetilde{G}_M = G_M + \delta G_M$, in which case the reduced cross section, up to order α^2 corrections, can be written [11]

$$\widetilde{\sigma}_R = G_M^2 + \frac{\varepsilon}{\tau} G_E^2 + 2G_M^2 \mathcal{R}e\left\{\frac{\delta G_M}{G_M} + \varepsilon Y_{2\gamma}\right\} + \frac{2\varepsilon}{\tau} G_E^2 \mathcal{R}e\left\{\frac{\delta G_E}{G_E} + \frac{G_M}{G_E} Y_{2\gamma}\right\}, \quad (34)$$

where the form factor $\widetilde{F}_3$ has been expressed in terms of the ratio:

$$Y_{2\gamma} = \widetilde{\nu}\frac{\widetilde{F}_3}{G_M}, \quad (35)$$

with $\widetilde{\nu} \equiv K \cdot P/M^2 = \sqrt{\tau(1+\tau)(1+\varepsilon)/(1-\varepsilon)}$. We should emphasize that the generalized form factors are not observables, and therefore have no intrinsic physical meaning. Thus the magnitude and ε dependence of the generalized form factors will depend on the choice of parametrization of the generalized amplitude. For example, the axial parametrization introduces an effective axial vector coupling beyond Born level, and is written as [29]

$$\mathcal{M} = -i\frac{e^2}{q^2}\left\{\bar{u}(p_3)\gamma_\mu u(p_1)\, \bar{u}(p_4)\left(F_1'\gamma^\mu + F_2'\frac{i\sigma^{\mu\nu}q_\nu}{2M}\right) \times u(p_2) + G_A'\bar{u}(p_3)\gamma_\mu\gamma_5 u(p_1)\bar{u}(p_4)\gamma^\mu\gamma_5 u(p_2)\right\}. \quad (36)$$

Following Ref. [12], one finds the following relationships:

$$F_1' = \widetilde{F}_1 + \widetilde{\nu}\widetilde{F}_3, \quad (37)$$

$$F_2' = \widetilde{F}_2, \quad (38)$$

$$G_A' = -\tau\widetilde{F}_3. \quad (39)$$

In Fig. 6 we show the contributions of 2γ exchange to the (real parts of the) proton $\widetilde{G}_E$ and $\widetilde{G}_M$ form factors and the ratio $Y_{2\gamma}$ evaluated at $Q^2 = 1$, 3, and 6 GeV^2. One observes that the 2γ correction to $\widetilde{G}_M$ is large, with a positive slope in ε that increases with Q^2. The correction to $\widetilde{G}_E$ is similar to that for $\widetilde{G}_M$ at $Q^2 = 1$ GeV^2, but becomes shallower at intermediate ε values for larger Q^2. Both of these corrections are significantly larger than the $Y_{2\gamma}$ correction, which is weakly Q^2 dependent and has a small negative slope in ε at larger Q^2. The contribution to $Y_{2\gamma}$ is found to be about 5 times smaller than that extracted in phenomenological analyses [9] under the assumption that the entire form factor discrepancy is because of the new $\widetilde{F}_3$ contribution (see also Ref. [30]).

C. Comparison of e^+p to e^-p cross sections

Direct experimental evidence for the contribution of 2γ exchange can be obtained by comparing e^+p and e^-p cross sections through the ratio:

$$R^{e^+e^-} \equiv \frac{d\sigma^{(e^+)}}{d\sigma^{(e^-)}} \approx \frac{\left|\mathcal{M}_0^{(e^+)}\right|^2 + 2\mathcal{R}e\left\{\mathcal{M}_0^{(e^+)\dagger}\mathcal{M}^{2\gamma(e^+)}\right\}}{\left|\mathcal{M}_0^{(e^-)}\right|^2 + 2\mathcal{R}e\left\{\mathcal{M}_0^{(e^-)\dagger}\mathcal{M}^{2\gamma(e^-)}\right\}}. \quad (40)$$

Whereas the Born amplitude $\mathcal{M}_0$ changes sign under the interchange $e^- \leftrightarrow e^+$, the 2γ exchange amplitude $\mathcal{M}^{2\gamma}$ does not. The interference of the $\mathcal{M}_0$ and $\mathcal{M}^{2\gamma}$ amplitudes therefore has the opposite sign for electron and positron scattering. Because the finite part of the 2γ contribution is negative over

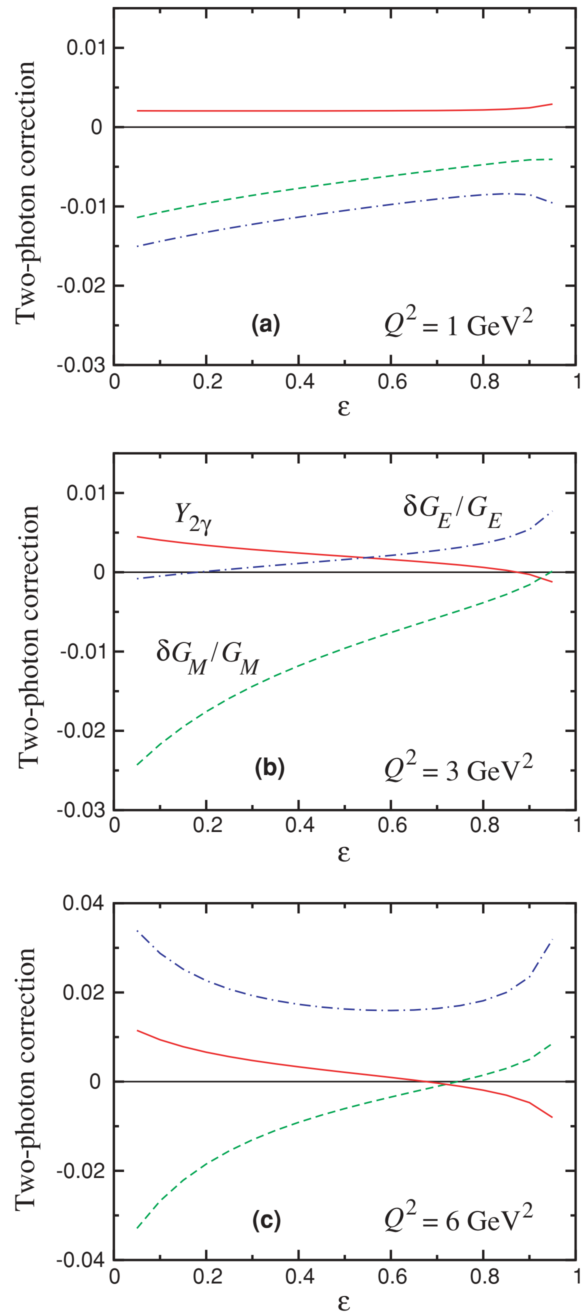

FIG. 6. (Color online) Finite 2γ contributions (defined with respect to the Mo-Tsai IR result [13]) to the real parts of the G_M (dashed), G_E (dot-dashed), and $Y_{2\gamma}$ (solid) form factors of the proton at $Q^2 = 1$, 3, and 6 GeV^2. Note the larger scale in the bottom figure.

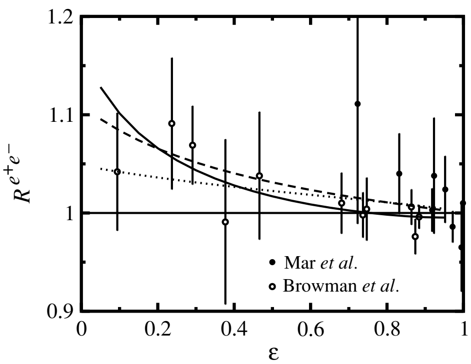

FIG. 7. Ratio of elastic e^+p to e^-p cross sections. The data are from SLAC [31,32], with Q^2 ranging from 0.01 to 5 GeV^2. The results of the 2γ exchange calculations are shown by the curves for $Q^2 = 1$ (dotted), 3 (dashed), and 6 GeV^2 (solid).

most of the range of ε, one would expect to see an enhancement of the ratio of e^+ to e^- cross sections,

$$R^{e^+e^-} \approx 1 - 2\Delta, \tag{41}$$

where Δ is defined in Eq. (27).

Although the current data on elastic e^-p and e^+p scattering are sparse, there are some experimental constraints from old data taken at SLAC [31,32], Cornell [33], DESY [34], and Orsay [35] (see also Ref. [36]). The data are predominantly at low Q^2 and at forward scattering angles, corresponding to large ε ($\varepsilon \lesssim 0.7$), where the 2γ exchange contribution is small ($\lesssim$1%). Nevertheless, the overall trend in the data reveals a small enhancement in $R^{e^+e^-}$ at the lower ε values, as illustrated in Fig. 7 (which shows a subset of the data, from the SLAC experiments [31,32]).

The data in Fig. 7 are compared with our theoretical results, calculated for several fixed values of Q^2 ($Q^2 = 1$, 3, and 6 GeV^2). The results are in good agreement with the data, although the errors on the data points are quite large. Clearly better quality data at backward angles, where an enhancement of up to $\sim$10% is predicted, would be needed for a more definitive test of the 2γ exchange mechanism. An experiment [37] using a beam of e^+e^- pairs produced from a secondary photon beam at Jefferson Lab will make simultaneous measurements of e^-p and e^+p elastic cross sections up to $Q^2 \sim 2$ GeV^2. A proposal to perform a precise ($\sim$1%) comparison of e^-p and e^+p scattering at $Q^2 = 1.6$ GeV^2 and $\varepsilon \approx 0.4$ has also been made at the VEPP-3 storage ring [38].

III. POLARIZED ELECTRON-PROTON SCATTERING

The results of the 2γ exchange calculation in the previous section give a clear indication of a sizable correction to the LT-separated data at moderate and large Q^2. The obvious question that arises is whether, and to what extent, the 2γ exchange affects the polarization transfer results, which show the dramatic falloff of the G_E^p/G_M^p ratio at large Q^2. In this section we examine this problem in detail.

The polarization transfer experiment involves the scattering of longitudinally polarized electrons from an unpolarized proton target, with the detection of the polarization of the recoil proton, $\vec{e} + p \to e + \vec{p}$. (The analogous process whereby a polarized electron scatters elastically from a polarized proton leaving an unpolarized final state gives rise to essentially the same information.) In the Born approximation the spin-dependent amplitude is given by

$$\mathcal{M}_0(s_1, s_4) = -i\frac{e^2}{q^2}\bar{u}(p_3)\gamma_\mu u(p_1, s_1)\bar{u}(p_4, s_4)\Gamma^\mu(q)u(p_2), \tag{42}$$

where $s_1 = (s_1^0; \vec{s}_1)$ and $s_4 = (s_4^0; \vec{s}_4)$ are the spin four-vectors of the initial electron and final proton, respectively, and the spinor $u(p_1, s_1)$ is defined such that $u(p_1, s_1)\bar{u}(p_1, s_1) = (\not{p}_1 + m)(1 + \gamma_5 \not{s}_1)/2$ and similarly for $\bar{u}(p_4, s_4)$. The spin four-vector (for either the electron or recoil proton) can be written in terms of the three-dimensional spin vector ζ specifying the spin direction in the rest frame (see, e.g., Ref. [39]),

$$s^\mu = \left(\frac{\vec{\zeta}\cdot\vec{p}}{m}; \vec{\zeta} + \vec{p}\frac{\vec{\zeta}\cdot\vec{p}}{m(m+E)}\right), \tag{43}$$

where m and E are the mass and energy of the electron or proton. Clearly in the limit $\vec{p} \to 0$, the spin four-vector $s \to (0; \vec{\zeta})$. Because ζ is a unit vector, one has $\vec{\zeta}^2 = 1$, and one can verify from Eq. (43) that $s^2 = -1$ and $p \cdot s = 0$. If the incident electron energy E_1 is much larger than the electron mass m, the electron spin four-vector can be related to the electron helicity $h = \vec{\zeta}_1 \cdot \vec{p}_1$ by

$$s_1 \approx h\frac{p_1}{m}. \tag{44}$$

The coordinate axes are chosen so that the recoil proton momentum $\vec{p}_4$ defines the z axis, in which case for longitudinally polarized protons one has $\vec{\zeta} = \hat{p}_4$. In the 1γ exchange approximation the elastic cross section for scattering a longitudinally polarized electron with a recoil proton polarized longitudinally is then given by

$$\frac{d\sigma^{(L)}}{d\Omega} = h\,\sigma_{\mathrm{Mott}}\frac{E_1 + E_3}{M}\sqrt{\frac{\tau}{1+\tau}}\tan^2\frac{\theta}{2}G_M^2. \tag{45}$$

For transverse recoil proton polarization we define the x axis to be in the scattering plane, $\hat{x} = \hat{y} \times \hat{z}$, where $\hat{y} = \hat{p}_1 \times \hat{p}_3$ defines the direction perpendicular, or normal, to the scattering plane. The elastic cross section for producing a transversely polarized proton in the final state, with $\vec{\zeta} \cdot \vec{p}_4 = 0$, is given by

$$\frac{d\sigma^{(T)}}{d\Omega} = h\,\sigma_{\mathrm{Mott}}2\sqrt{\frac{\tau}{1+\tau}}\tan\frac{\theta}{2}G_E G_M. \tag{46}$$

Taking the ratio of the transverse to longitudinal proton cross sections then gives the ratio of the electric to magnetic proton form factors, as in Eq. (5). Note that in the 1γ exchange approximation the normal polarization is identically zero.

The amplitude for the 2γ exchange diagrams in Fig. 1 with the initial electron and final proton polarized can be written as follows:

$$\mathcal{M}^{2\gamma}(s_1, s_4) = e^4 \int \frac{d^4k}{(2\pi)^4} \frac{N_{\text{box}}(k, s_1, s_4)}{D_{\text{box}}(k)} + e^4 \int \frac{d^4k}{(2\pi)^4} \frac{N_{\text{x-box}}(k, s_1, s_4)}{D_{\text{x-box}}(k)}, \quad (47)$$

where the numerators are the matrix elements

$$N_{\text{box}}(k, s_1, s_4) = \bar{u}(p_3)\gamma_\mu(\not{p}_1 - \not{k} + m)\gamma_\nu u(p_1, s_1)\bar{u}(p_4, s_4) \times \Gamma^\mu(q-k)(\not{p}_2 + \not{k} + M)\Gamma^\nu(k)u(p_2), \quad (48)$$

$$N_{\text{x-box}}(k, s_1, s_4) = \bar{u}(p_3)\gamma_\nu(\not{p}_3 + \not{k} + m)\gamma_\mu u(p_1, s_1)\bar{u}(p_4, s_4) \times \Gamma^\mu(q-k)(\not{p}_2 + \not{k} + M)\Gamma^\nu(k)u(p_2), \quad (49)$$

and the denominators are given in Eqs. (17) and (18). The traces in Eqs. (48) and (49) can be evaluated using the explicit expression for the spin-vectors s_1 and s_4 in Eqs. (43) and (44).

In analogy with the unpolarized case [see Eq. (27)], the spin-dependent corrections to the longitudinal (Δ_L) and transverse (Δ_T) cross sections are defined as the finite parts of the 2γ contributions relative to the IR expression from Mo and Tsai [13] in Eq. (23), which are independent of polarization,

$$\Delta_{L,T} = \delta^{\text{full}}_{L,T} - \delta_{\text{IR}}. \quad (50)$$

Experimentally, one does not usually measure the longitudinal or transverse cross section *per se*, but rather the ratio of the transverse or longitudinal cross section to the unpolarized cross section, denoted P_L or P_T, respectively. Thus the 2γ exchange correction to the polarization transfer ratio can be incorporated as

$$\frac{P^{1\gamma+2\gamma}_{L,T}}{P^{1\gamma}_{L,T}} = \frac{1+\Delta_{L,T}}{1+\Delta}, \quad (51)$$

where Δ is the correction to the unpolarized cross section considered in the previous section.

The 2γ exchange contribution relative to the Born term is shown in Fig. 8. The correction to the longitudinal polarization transfer ratio P_L is small overall. This is because the correction Δ_L to the longitudinal cross section is roughly the same as the correction Δ to the unpolarized cross section. The corrections Δ and Δ_L must be exactly the same at $\theta = 180^\circ$ ($\varepsilon = 0$), and our numerical results bear this out. By contrast, the correction to the transverse polarization transfer ratio P_T is enhanced at backward angles and grows with Q^2. This is because of a combined effect of Δ_T becoming more positive with increasing Q^2 and Δ becoming more negative.

In the standard radiative corrections using the results of Mo and Tsai [13], the corrections for transverse polarization are the same as those for longitudinal polarization, so that no additional corrections beyond hard bremsstrahlung need be applied [39]. Because the polarization transfer experiments [5] typically have $\varepsilon \approx 0.7$–0.8, the shift in the polarization transfer ratio in Eq. (5) due to 2γ exchange corrections is not expected to be dramatic. If R is the corrected ("true") electric to magnetic form factor ratio, as in Eq. (29), then the measured polarization

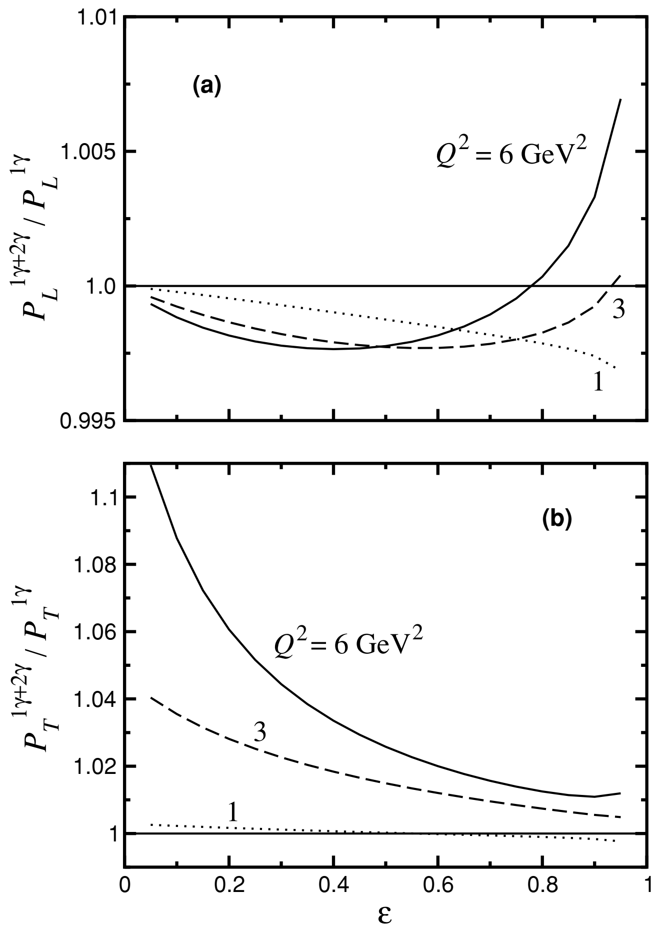

FIG. 8. Ratio of the finite part [with respect to the IR contribution in Eq. (22)] of the Born+2γ correction relative to the Born term, for (a) longitudinal and (b) transverse recoil proton polarization, at $Q^2 = 1$ (dotted), 3 (dashed), and 6 GeV^2 (solid). Note the different scales on the vertical axes.

transfer ratio is

$$\widetilde{R} = R\left(\frac{1+\Delta_T}{1+\Delta_L}\right). \quad (52)$$

Inverting Eq. (52), the shift in the ratio R is illustrated in Fig. 9 by the solid circles (offset slightly for clarity). The unshifted results are indicated by the open circles, and the LT separated results are labeled by diamonds. The effect of the 2γ exchange on the form factor ratio is a very small, $\lesssim 3\%$ suppression of the ratio at the larger Q^2 values, which is well within the experimental uncertainties.

Note that the shift in R in Eq. (52) does not include corrections from hard photon bremsstrahlung (which are part of the standard radiative corrections). Because these would make both the numerator and denominator in Eq. (52) even larger, the correction shown in Fig. 9 would represent an upper limit on the shift in R.

Finally, the 2γ exchange process can give rise to a nonzero contribution to the elastic cross section for a recoil proton polarized normal to the scattering plane. This contribution is purely imaginary, and does not exist in the 1γ exchange

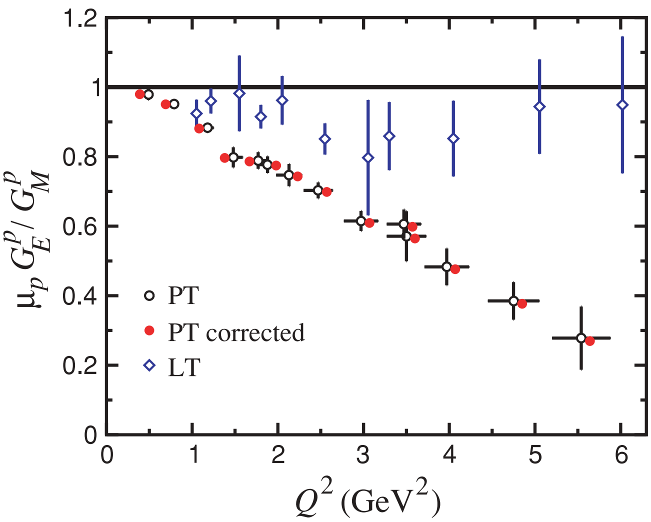

FIG. 9. (Color online) Proton electric to magnetic form factor ratio obtained from the polarization transfer measurements [5], with (solid circles) and without (open circles) the 2γ exchange corrections. The corrected values have been offset for clarity. The LT-separated ratio (open diamonds) from Fig. 5 is shown for comparison.

approximation. It is illustrated in Fig. 10, where the ratio Δ_N of the 2γ exchange contribution relative to the *unpolarized* Born contribution is shown as a function of ε for several values of Q^2. (For consistency in notation we denote this correction Δ_N rather than δ_N, even though there is no IR contribution to the normal polarization.)

The normal polarization contribution is very small numerically, $\Delta_N \lesssim 1\%$, and has a very weak ε dependence. In contrast to Δ_L and Δ_T, the normal polarization ratio is smallest at low ε, becoming larger with increasing ε. Although not directly relevant to the elastic form factor extraction, the observation of protons with normal polarization would provide direct evidence of 2γ exchange in elastic scattering. Figure 11

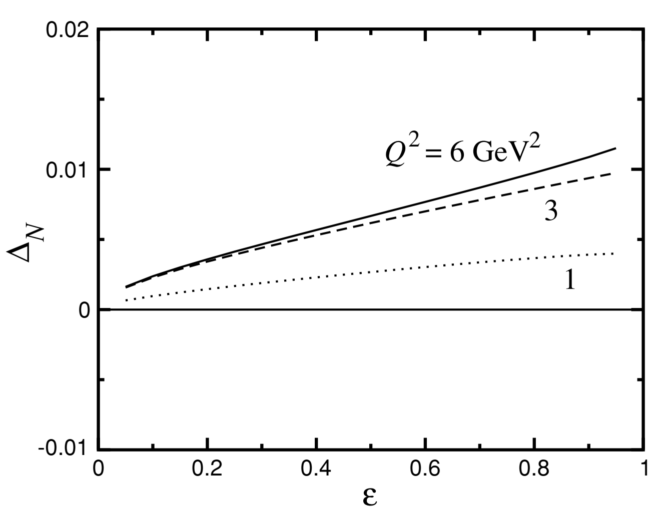

FIG. 10. Ratio of the 2γ contribution to the normal polarization, to the unpolarized Born contribution, as a function of ε, for $Q^2 = 1$ (dotted), 3 (dashed), and 6 GeV^2 (solid).

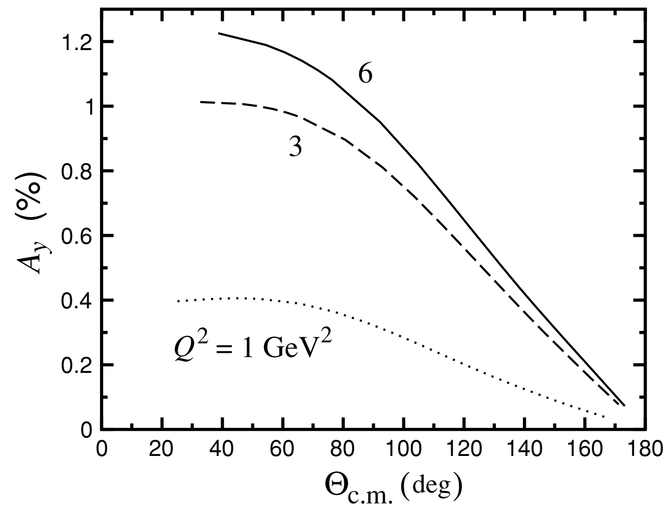

FIG. 11. Normal polarization asymmetry, expressed as a percentage, as a function of the center-of-mass scattering angle, $\Theta_{\rm cm}$, for $Q^2 = 1$ (dotted), 3 (dashed), and 6 GeV^2 (solid).

shows the normal polarization asymmetry A_y as a function of the center-of-mass scattering angle, $\Theta_{\rm cm}$, for several values of Q^2. The asymmetry is relatively small, of the order of 1% at small $\Theta_{\rm cm}$ for $Q^2 \sim 3$ GeV^2, but grows with Q^2.

The imaginary part of the 2γ amplitude can also be accessed by measuring the electron beam asymmetry for electrons polarized normal to the scattering plane [40]. Knowledge of the imaginary part of the 2γ exchange amplitude could be used to constrain models of Compton scattering, although relating this to the real part (as needed for form factor studies) would require a dispersion relation analysis.

IV. ELECTRON-NEUTRON SCATTERING

In this section we examine the effect of the 2γ exchange contribution on the form factors of the neutron. Because the magnitude of the electric form factor of the neutron is relatively small compared with that of the proton, and as we saw in Sec. III the effects on the proton are significant at large Q^2, it is important to investigate the extent to which G_E^n may be contaminated by 2γ exchange.

Using the same formalism as in Secs. II and III, the calculated 2γ exchange correction for the neutron is shown in Fig. 12 for $Q^2 = 1$, 3, and 6 GeV^2. Because there is no IR divergent contribution to δ for the neutron, the total 2γ correction $\delta^{\rm full}$ is displayed in Fig. 12. In the numerical calculation, the input neutron form factors from Ref. [16] are parametrized using the pole fit in Eq. (26), with the parameters given in Table I. For comparison, the correction at $Q^2 = 6$ GeV^2 is also computed using a 3-pole fit to the form factor parametrization from Ref. [41]. The difference between these is an indication of the model dependence of the calculation.

The most notable difference with respect to the proton results is the sign and slope of the 2γ exchange correction. Namely, the magnitude of the correction $\delta^{\rm full}(\varepsilon, Q^2)$ for the neutron is $\sim$3 times smaller than for the proton. The reason for

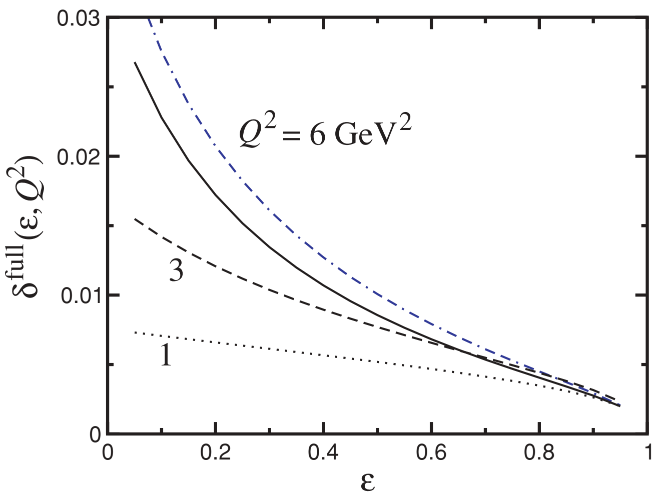

FIG. 12. (Color online) 2γ contribution to the unpolarized electron-neutron elastic scattering cross section, at $Q^2 = 1$ (dotted), 3 (dashed), and 6 GeV^2 (solid and dot-dashed). The dot-dashed curve corresponds to the form factor parametrization of Ref. [41], whereas the others are from Ref. [16] (as fitted by the parameters in Table I).

the sign change is the negative anomalous magnetic moment of the neutron. The ε dependence is approximately linear at moderate and high ε, but at low ε there exists a clear deviation from linearity, especially at large Q^2.

Translating the ε dependence to the form factor ratio, the resulting shift in $\mu_n G_E^n / G_M^n$ is shown in Fig. 13 at several values of Q^2, assuming a linear 2γ correction over two different ε ranges ($\varepsilon = 0.2 - 0.9$ and $\varepsilon = 0.5 - 0.8$). The baseline (uncorrected) data are from the global fit in Ref. [16]. The shift due to 2γ exchange is small at $Q^2 = 1$ GeV^2, but increases significantly by $Q^2 = 6$ GeV^2, where it produces a 50–60% rise in the uncorrected ratio. These results

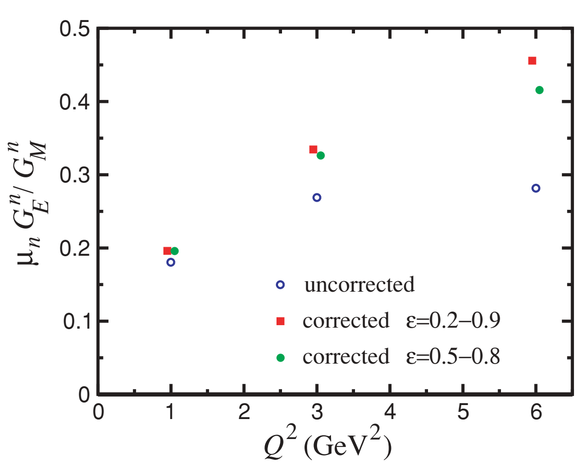

FIG. 13. (Color online) Effect of 2γ exchange on the ratio of neutron form factors $\mu_n G_E^n / G_M^n$ using LT separation. The uncorrected points (open circles) are from the form factor parametrization in Ref. [16], whereas the points corrected for 2γ exchange are obtained from linear fits to $\delta^{\rm full}$ in Fig. 12 for $\varepsilon = 0.2 - 0.9$ (filled squares) and $\varepsilon = 0.5 - 0.8$ (filled circles) (offset for clarity).

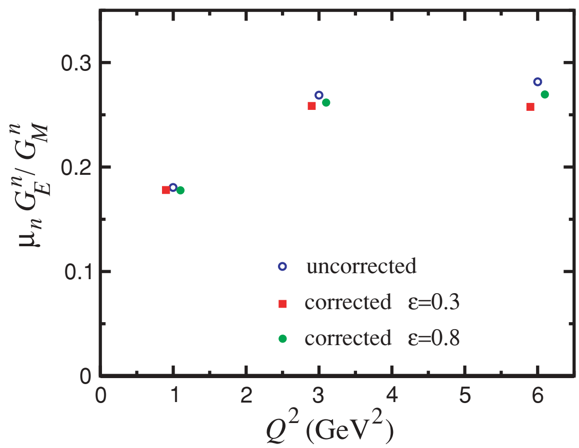

FIG. 14. (Color online) Effect of 2γ exchange on the ratio of neutron form factors $\mu_n G_E^n / G_M^n$ using polarization transfer. The uncorrected points (open circles) are from the parametrization in Ref. [16], and the points corrected for 2γ exchange correspond to $\varepsilon = 0.3$ (filled squares) and $\varepsilon = 0.8$ (filled circles) (offset for clarity).

suggest that, as for the proton, the LT separation method is subject to large corrections from 2γ exchange at large Q^2.

Although the 2γ corrections to the form factor ratio from LT separation are significant, particularly at large Q^2, in practice the neutron G_E^n form factor is commonly extracted using the polarization transfer method. To compare the 2γ effects on the ratio $\mu_n G_E^n / G_M^n$ extracted by polarization transfer, in Fig. 14 we plot the same "data points" as in Fig. 13, shifted by the $\delta_{L,T}$ corrections as in Eq. (52) at two values of ε ($\varepsilon = 0.3$ and 0.8). The shift is considerably smaller than that from the LT method but nevertheless represents an approximately 4% (3%) suppression at $\varepsilon = 0.3$ (0.8) for $Q^2 = 3$ GeV^2 and $\approx$10% (5%) suppression for $Q^2 = 6$ GeV^2 for the same ε. In the Jefferson Lab experiment [42] to measure G_E^n / G_M^n at $Q^2 = 1.45$ GeV^2 the value of ε was around 0.9, at which the 2γ correction was $\approx$2.5%. In the recently approved extension of this measurement to $Q^2 \approx 4.3$ GeV^2 [43], the 2γ correction for $\varepsilon \approx 0.82$ is expected to be around 3%. Although small, these corrections will be important to take into account to achieve precision at the several-percent level. Furthermore, the two-photon exchange effects may also need to be taken into account when extracting the neutron magnetic form factor G_M^n from cross-section data.

V. ^{3}HE ELASTIC FORM FACTORS

In this section we extend our formalism to the case of elastic scattering from ^{3}He nuclei. Of course, the contribution of ^{3}He intermediate states in 2γ exchange is likely to constitute only a part of the entire effect – contributions from breakup channels may also be important. However, we can obtain an estimate on the size of the effect on the ^{3}He form factors, in comparison with the effect on the nucleon form factor ratio.

The expressions used to evaluate the 2γ contributions are similar to those for the nucleon, because ^{3}He is a spin-$\frac{1}{2}$ particle, although there are some important differences. For instance, the charge is now Ze (where $Z = 2$ is the atomic

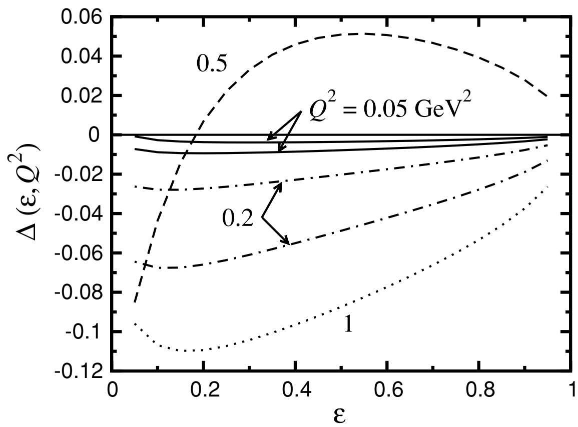

FIG. 15. 2γ contribution to the unpolarized electron-^{3}He elastic scattering cross section, with the ^{3}He elastic intermediate state, as a function of ε, for $Q^2 = 0.05$ (solid), 0.2 (dot-dashed), 0.5 (dashed), and 1 GeV^2 (dotted). A parametrization of the form factor from Ref. [44] is used in all cases, except for the upper solid and dot-dashed curves, for which a dipole shape with mass $\Lambda_{^3\mathrm{He}} = 0.37$ GeV is used.

number of ^{3}He), the mass $M_{^3\mathrm{He}}$ is $\approx$3 times larger than the nucleon mass, and the anomalous magnetic moment is $\kappa_{^3\mathrm{He}} = -4.185$. In addition, the internal γ^3He form factors are somewhat softer than the corresponding nucleon form factor (because the charge radius of the ^{3}He nucleus is $\approx$1.88 fm) and have zeros at $Q^2 \approx 0.45$ and 0.7 GeV^2 for the charge (F_C) and magnetic (F_M) form factors, respectively [44]. (Analyzing the ratio F_C/F_M is not meaningful therefore because of the zero in F_M.)

Using a three-monopole fit [45] to the ^{3}He form factors from Amroun *et al.* [44], the 2γ exchange correction Δ is shown in Fig. 15 as a function of ε for several values of Q^2. As for the proton, Δ is negative at low Q^2, and generally increases in magnitude with increasing Q^2. However, there are several important differences between the ^{3}He and proton cases. First, the larger charge squared Z^2 of the ^{3}He nucleus makes the effect larger (by a factor $\sim$4), whereas the larger mass squared of the ^{3}He nucleus suppresses the effect by a factor $\sim$9. In addition, the form factor at low Q^2 is much softer than that of the nucleon. However, the main difference stems from the presence of the zeros in the form factors at $Q^2 \sim 0.5$ GeV^2, which gives rise to the dramatic change of sign in Δ at $Q^2 = 0.5$ GeV^2.

To estimate the model dependence of the results, we have also calculated the correction Δ assuming a dipole shape with a cutoff mass $\Lambda_{^3\mathrm{He}} = 0.37$ GeV, fitted to the ^{3}He radius, which gives a reasonable approximation at low Q^2 ($\lesssim$0.05 GeV^2). The results with this form factor, indicated by the upper curves for $Q^2 = 0.05$ and 0.2 GeV^2 in Fig. 15, are about a factor 2 smaller in magnitude than for the form factor from Ref. [44]. Using the value $\Lambda_{^3\mathrm{He}} = 0.34$ GeV, which underestimates the form factor at low Q^2, but gives a better overall fit at higher Q^2 ($\lesssim$0.1 GeV^2), leads to similar results as those for $\Lambda_{^3\mathrm{He}} =$ 0.37 GeV. At larger Q^2 the dipole shape is not a good representation of the ^{3}He form factor, and it is difficult to estimate the model dependence of Δ. These results therefore illustrate the potential relevance of two-photon exchange effects for future ^{3}He form-factor measurements, which will extend the Q^2 range to $Q^2 \approx 4$ GeV^2 [46].

VI. CONCLUSION

We have presented a comprehensive analysis of the effects of 2γ exchange in elastic electron-nucleon scattering, taking particular account of the effects of nucleon structure. Our main purpose has been to quantify the 2γ effect on the ratio of electric to magnetic form factors of the proton, which has generated controversy recently stemming from conflicting results of measurements at large Q^2.

Consistent with the earlier preliminary investigation [10], we find that inclusion of 2γ exchange reduces the G_E^p/G_M^p ratio extracted from LT-separated cross section data, and resolves a significant amount of the discrepancy with the polarization transfer results. At higher Q^2 we find strong deviations from linearity, especially at small ε, which can be tested in future high-precision cross section measurements. There is some residual model dependence in the calculation of the 2γ amplitude arising from the choice of form factors at the internal $\gamma^* NN$ vertices in the loop integration. This dependence, although not overwhelming, will place limitations on the reliability of the LT separation technique in extracting high-Q^2 form factors. However, the size of the 2γ contributions to elastic scattering could be determined from measurement of the ratio of $e^- p$ to $e^+ p$ elastic cross sections, which are uniquely sensitive to 2γ exchange effects.

We have also generalized our analysis to the case where the initial electron and recoil proton are polarized, as in the polarization transfer experiments. Although the 2γ corrections can be as large as $\sim$4–5% at small ε for $Q^2 \sim 6$ GeV^2, because the polarization transfer measurements are performed typically at large ε we find the impact on the extracted G_E^p/G_M^p ratio to be quite small, amounting to $\lesssim$3% suppression at the highest Q^2 value. However, future measurements at higher Q^2 will go to lower ε values, so that the 2γ effects will need to be taken into account to achieve precision at the several-percent level, especially if the G_E^p/G_M^p ratio continues to fall with Q^2.

Extending the formalism to the case of the neutron, we have calculated the 2γ exchange corrections to the neutron G_E^n/G_M^n ratio. Although numerically smaller than for the proton, the corrections are nonetheless important because the magnitude of G_E^n itself is small compared with G_E^p. Furthermore, because of the opposite sign of the neutron magnetic moment relative to the proton, the 2γ corrections to the LT-separated cross section give rise to a sizable enhancement of G_E^n/G_M^n at large Q^2. The analogous effects for the polarization transfer ratio are small, however, giving rise to a few percent suppression for $Q^2 \lesssim 6$ GeV^2.

Finally, we have also obtained an estimate of the 2γ exchange contribution to the elastic form factors of ^{3}He from elastic intermediate states. At low Q^2 the two-photon exchange correction is negative and generally increases in magnitude with increasing Q^2, as for the proton. However, the presence of zeros in the ^{3}He form factors at $Q^2 \sim 0.5$ GeV^2

gives rise to nonmonotonic behavior and reveals potentially interesting two-photon exchange effects in future ^{3}He form factor measurements at larger Q^2 [46].

Contributions from excited states, such as the Δ and heavier baryons, may modify the quantitative analysis presented here. Naively, one could expect their effect to be suppressed because of the larger masses involved, at least for the real parts of the form factors. An investigation of the inelastic excitation effects is presented in Ref. [14].

ACKNOWLEDGMENTS

We thank J. Arrington for helpful discussions and comments on the manuscript and R. Feuerbach for his ^{3}He form factor parametrization. This work was supported in part by NSERC (Canada), DOE grant DE-FG02-93ER-40762, and DOE contract DE-AC05-84ER-40150 under which the Southeastern Universities Research Association (SURA) operates the Thomas Jefferson National Accelerator Facility (Jefferson Lab).

[1] R. C. Walker *et al*., Phys. Rev. D **49**, 5671 (1994).
[2] J. Arrington, Phys. Rev. C **68**, 034325 (2003).
[3] M. E. Christy *et al*., Phys. Rev. C **70**, 015206 (2004).
[4] I. A. Qattan *et al*., Phys. Rev. Lett. **94**, 142301 (2005); J. Arrington, arXiv:nucl-ex/0312017.
[5] M. K. Jones *et al*., Phys. Rev. Lett. **84**, 1398 (2000); O. Gayou *et al*., Phys. Rev. Lett. **88**, 092301 (2002); V. Punjabi *et al*., Phys. Rev. C **71**, 055202 (2005) [Erratum-*ibid.* **71**, 069902 (2005)].
[6] G. P. Lepage and S. J. Brodsky, Phys. Rev. D **22**, 2157 (1980); V. L. Chernyak and A. R. Zhitnitsky, Sov. J. Nucl. Phys. **31**, 544 (1980) [Yad. Fiz. **31**, 1053 (1980)].
[7] P. Jain and J. P. Ralston, Pramana **61**, 987 (2003).
[8] A. V. Belitsky, X. Ji, and F. Feng-Yuan, Phys. Rev. Lett. **91**, 092003 (2003).
[9] P. A. M. Guichon and M. Vanderhaeghen, Phys. Rev. Lett. **91**, 142303 (2003).
[10] P. G. Blunden, W. Melnitchouk, and J. A. Tjon, Phys. Rev. Lett. **91**, 142304 (2003).
[11] Y. C. Chen, A. Afanasev, S. J. Brodsky, C. E. Carlson, and M. Vanderhaeghen, Phys. Rev. Lett. **93**, 122301 (2004).
[12] A. V. Afanasev, S. J. Brodsky, C. E. Carlson, Y. C. Chen, and M. Vanderhaeghen, Phys. Rev. D **72**, 013008 (2005).
[13] L. W. Mo and Y. S. Tsai, Rev. Mod. Phys. **41**, 205 (1969); Y. S. Tsai, Phys. Rev. **122**, 1898 (1961).
[14] S. Kondratyuk, P. G. Blunden, W. Melnitchouk, and J. A. Tjon, arXiv:nucl-th/0506026, to appear in Phys. Rev. Lett.
[15] L. C. Maximon and J. A. Tjon, Phys. Rev. C **62**, 054320 (2000).
[16] P. Mergell, U. G. Meissner, and D. Drechsel, Nucl. Phys. **A596**, 367 (1996).
[17] J. A. M. Vermaseren, *New Features of FORM*, arXiv:math-ph/0010025.
[18] M. Jamin and M. E. Lautenbacher, *Tracer: Mathematica Package for Gamma-Algebra in Arbitrary Dimensions*, http://library.wolfram.com/infocenter/Articles/3129/.
[19] R. Mertig, M. Bohm, and A. Denner, Comput. Phys. Commun. **64**, 345 (1991), http://www.feyncalc.org.
[20] T. Hahn and M. Perez-Victoria, Comput. Phys. Commun. **118**, 153 (1999), http://www.feynarts.de.
[21] G. Passarino and M. J. Veltman, Nucl. Phys. **B160**, 151 (1979).
[22] G. 't Hooft and M. J. Veltman, Nucl. Phys. **B153**, 365 (1979).
[23] M. J. Veltman, *FORMF*, *A Program for the Numerical Evaluation of Form Factors* (Utrecht, 1979).
[24] G. J. van Oldenborgh and J. A. M. Vermaseren, Z. Phys. C **46**, 425 (1990), http://www.nikhef.nl/~t68/ff.
[25] J. Arrington, Phys. Rev. C **69**, 022201(R) (2004).
[26] E. J. Brash, A. Kozlov, S. Li, and G. M. Huber, Phys. Rev. C **65**, 051001(R) (2002).
[27] L. Andivahis *et al*., Phys. Rev. D **50**, 5491 (1994).
[28] Jefferson Lab experiment E05-017, *A Measurement of Two-Photon Exchange in Unpolarized Elastic Electron-Proton Scattering*, J. Arrington, spokesperson.
[29] M. P. Rekalo and E. Tomasi-Gustafsson, Nucl. Phys. **A742**, 322 (2004).
[30] J. Arrington, Phys. Rev. C **71**, 015202 (2005).
[31] A. Browman, F. Liu, and C. Schaerf, Phys. Rev. **139**, B1079 (1965).
[32] J. Mar *et al*., Phys. Rev. Lett. **21**, 482 (1968).
[33] R. L. Anderson *et al*., Phys. Rev. Lett. **17**, 407 (1966); Phys. Rev. **166**, 1336 (1968).
[34] W. Bartel *et al*., Phys. Lett. **B25**, 242 (1967).
[35] B. Bouquet *et al*., Phys. Lett. **B26**, 178 (1968).
[36] J. Arrington, Phys. Rev. C **69**, 032201(R) (2004).
[37] Jefferson Lab experiment E04-116, *Beyond the Born Approximation: A Precise Comparison of* e^+p *and* e^-p *Scattering in CLAS*, W. K. Brooks *et al*., spokespersons.
[38] J. Arrington *et al*., *Two-Photon Exchange and Elastic Scattering of Electrons/Positrons on the Proton*, proposal for an experiment at VEPP-3 (2004), arXiv:nucl-ex/0408020.
[39] L. C. Maximon and W. C. Parke, Phys. Rev. C **61**, 045502 (2000).
[40] S. P. Wells *et al*., Phys. Rev. C **63**, 064001 (2001); F. E. Maas *et al*., Phys. Rev. Lett. **94**, 082001 (2005).
[41] P. E. Bosted, Phys. Rev. C **51**, 409 (1995).
[42] R. Madey *et al*., Phys. Rev. Lett. **91**, 122002 (2003).
[43] Jefferson Lab experiment E04-110, *The Neutron Electric Form Factor at* $Q^2 = 4.3$ *(GeV/c)*^{2} *from the Reaction* $^2H(\vec{e}, e'\vec{n})^1H$ *via Recoil Polarimetry*, R. Madey, spokesperson.
[44] A. Amroun *et al*., Nucl. Phys. **A579**, 596 (1994).
[45] R. Feuerbach, private communication.
[46] Jefferson Lab experiment E04-018, *Elastic Electron Scattering off* ^{3}*He and* ^{4}*He at Large Momentum Transfers*, J. Gomez, A. Katramatou, and G. Petratos, spokespersons.